


Original article

Anomalous Variations of the Typhoon Lionrock Induced Inertial Oscillations of Shelf Waters in the Peter the Great Bay in August – September, 2016

V. V. Novotryasov , A. A. Sergeev, E. P. Pavlova

*V. I. Il'ichev Pacific Oceanological Institute, Far Eastern Branch of Russian Academy of Sciences,
Vladivostok, Russian Federation*

 *vadimnov@poi.dvo.ru*

Abstract

Purpose. The purpose of the study is to analyze the characteristics of inertial oscillations induced by extreme atmospheric effects against the background of the shear current, using the example of inertial oscillations caused by the typhoon Lionrock in the shelf waters of the southwestern Peter the Great Bay against the background of the near-slope Primorskoe current.

Methods and Results. The frequency-temporal spectral analysis of the typhoon Lionrock induced mesoscale variability of the rotational components' realizations of the current velocity vector was applied. The current velocity realizations were obtained using the Seawatch oceanographic system moored on the southwestern shelf of the Peter the Great Bay. The specified analysis made it possible to establish that at the latitude at which the Seawatch system had been installed and at the initial stage of the typhoon impact, the spectral density of currents kinetic energy grew significantly at clockwise rotation at frequency ω , close to the Coriolis parameter $f \approx 2\pi/18$ (rad/h). A similar growth of the kinetic energy spectral density was recorded at the same frequency ω , but at the counterclockwise rotation and at the final stage of typhoon impact. The recorded inertial oscillations of velocity vector at opposite directions of its rotation at frequency ω , demonstrate a significant difference of their travel time curves from the canonical one at a circular clockwise rotation.

Conclusions. Against the background of the near-slope Primorskoe current significantly amplified (up to 0.9 m/s) by the typhoon Lionrock, the velocity inertial variations of this current induced by the typhoon on the shelf of the Peter the Great Bay, show anomalous variability. The model of these oscillations in the presence of a shear current proposed by G. K. Korotaev and K. D. Sabinin (2017) provides a qualitative interpretation of the inertial oscillations' variability in the bay shelf waters resulted from the typhoon Lionrock impact in August – September, 2016.

Keywords: inertial oscillations, velocity hodograph, shear current, field data, shelf, Peter the Great Bay, typhoon Lionrock, typhoon

Acknowledgements: The authors are grateful to the reviewer for the comments which favored a significant improvement of the article. The work was carried out within the framework of the theme of state assignment of POI FEB of RAS "Mathematical simulation and analysis of dynamic processes in the ocean" (theme No. 121021700341-2).

For citation: Novotryasov, V.V., Sergeev, A.A. and Pavlova, E.P., 2023. Anomalous Variations of the Typhoon Lionrock Induced Inertial Oscillations of Shelf Waters in the Peter the Great Bay in August – September, 2016. *Physical Oceanography*, 30(2), pp. 215-228. doi:10.29039/1573-160X-2023-2-215-228

DOI: 10.29039/1573-160X-2023-2-215-228

© V. V. Novotryasov, A. A. Sergeev, E. P. Pavlova, 2023

© Physical Oceanography, 2023

Introduction

Among the mesoscale oscillations with periods of many hours, a special place is occupied by inertial current velocity oscillations, which have periods close to $2\pi/f$ at a fixed latitude ($f = 2\Omega|\sin\phi|$ is the Coriolis parameter at this latitude) [1].



Oscillations with an inertial period represent circular rotation of seawater and are manifested in measurements of the current velocity at a given point, the vector of which rotates clockwise with a frequency equal to the value of the Coriolis parameter f at the observation latitude.

Wind-induced inertial oscillations (IO) are the subject of active study, since this motion plays an important role in the momentum transfer from the atmosphere to the oceans [2]. The excitation of IO under the action of wind stress in the upper mixed layer of the ocean has been widely studied using observations, analytical and numerical models. Notable observational results were obtained in the 1980s, for example, in [3, 4], and then in the pioneering work [5]. These studies have shown that fluctuations in the velocity of currents under the mixing layer are dominated by fluctuations of the quasi-inertial frequency, which are qualitatively consistent with the kinematics of internal waves.

At the center of the renewed (in the past decade) interest in quasi-inertial internal waves is the energy that these waves transfer to the inner layers of the ocean. It is assumed that most of this energy is dissipated in the surface layer of the ocean and used there for its mixing. In this regard, the share of the radiation flux in the surface energy flux is of particular interest to specialists in ocean modeling [6].

The IO studies are important not only for studying their features in water areas, including coastal ones, but also for analyzing the conditions for the distribution of pollution of natural and anthropogenic origin [7]. In addition, the study of the mechanisms and conditions for the IO generation and propagation in the shelf zone of the oceans is important for interpreting the results of ground-based space monitoring of marine areas [8, 9].

Based on long-term observations on the Hawaiian shelf and the subsequent analysis of the IO properties, published in [10, 11], a number of anomalous features of these oscillations was revealed. Among them, there is a shape of the velocity hodograph, the direction of its rotation, the periods of the velocity vector rotation, and a number of others. It was suggested that, near steep slopes and under effect of strong and spatially inhomogeneous currents, the IO characteristics may experience significant changes, and the observed distortions of the inertial current hodographs are a consequence of the superposition of the IO and the background shear current.

In a recent work by K.D. Sabinin and G.K. Korotaev [12], an analytical model of the current velocity IO in the presence of a background shear current was formulated based on the exact solution of the shallow water equations. Within the framework of this model, the assumption that the IO characteristics can experience significant changes under the effect of strong and inhomogeneous flows in space was substantiated. Using this model, an interpretation of the IO variability, recorded in the above-mentioned works, was given.

The main cause of IO is considered to be the wind effect [13]. In this regard, in this work, a study of the specific features of the shelf water IO caused by extreme atmospheric forcing, such as a typhoon, was carried out. The paper analyzes the features of the IO on the shelf of the Peter the Great Bay, which were formed under the effect of Typhoon Lionrock in August – September 2016.

The study was carried out using the velocity measurements of currents in the southwestern region of the bay using the Seawatch autonomous moored oceanographic measuring system. A preliminary analysis of the measurement data, performed in [14], showed that under effect of a typhoon in the area under study, not only currents with velocity fluctuations at frequencies close to the inertial frequency, but also the low-frequency synoptic component of the near-slope jet Primorskoe current were intensified.

The purpose of this work is to analyze the mesoscale variability of the current velocity caused by Typhoon Lionrock over the southwestern region shelf of the Peter the Great Bay, to characterize the IO caused by this typhoon, and to give a qualitative interpretation of the anomalous changes in the recorded IO, using the model of this movement in a current with a velocity shift [12].

To achieve this goal, the following problems were solved. Based on the measurement data, specific features of the current velocity IO in the bay were determined and evaluated before, during, and after the typhoon impact on the shelf waters of the bay. The analysis of inertial currents was carried out using non-standard time-frequency spectral analysis, which takes into account the rotational nature of these flows, based on the method of rotational components [15], as well as the non-stationary nature of the IO. The specified method determined the spectral density of the kinetic energy of rotation at a frequency close to the Coriolis parameter, the direction of the IO rotation, the shape and eccentricity of the hodograph of these flows. The listed characteristics of the IO obtained at the initial stage of maximum development and the final stage of the typhoon impact on the shelf waters of the bay are compared.

Description of the study area, data used and methods of their processing

The Peter the Great Bay is the largest bay in the northwestern region of the Sea of Japan. The length of the bay from north to south is about 80 km, the maximum width from west to east is ~ 200 km, and the average shelf depth is ~ 100 m. The bay is a mixing zone of the waters of the northern Primorskoe and southern North Korean jet near-slope currents [16].

In the last week of August 2016, the waters of the bay were under the effect of Typhoon Lionrock, which reached its maximum development in the period from 16:00 (hereinafter, local time) on August 28 to 10:00 on August 29 [17]. A few days earlier, a cyclone formed over the Sea of Japan, causing an increase in southerly winds over the waters of the bay ¹. Subsequently, the typhoon moved directly to the area of Peter the Great Bay. At 04:00 on August 31, the typhoon reached the coast of Primorsky Krai. The wind speed in the east direction reached its maximum. At 10:00 on August 31, Typhoon Lionrock and a cyclone that originated over the Sea of Japan merged into an area of low surface atmospheric pressure, which then moved to the mainland and began to fill rapidly.

¹ FERHRI, 2016. *Monthly Hydrometeorological Bulletin of FERHRI*. [online] Available at: http://ferhri.org/images/stories/FERHRI/Bulletins/Bul_2016.08_ch5_typhoon.pdf [Accessed: 20 July 2022].

As it is known, the main cause of inertial oscillations of the sea waters is wind. Fig. 1 demonstrates the realizations of the zonal V and the meridional U projections of the wind speed vector from 00:00 on August 20, 2016, recorded by the meteorological station of the hydrographic buoy, before, during and after the end of the typhoon impact on the shelf waters of the bay.

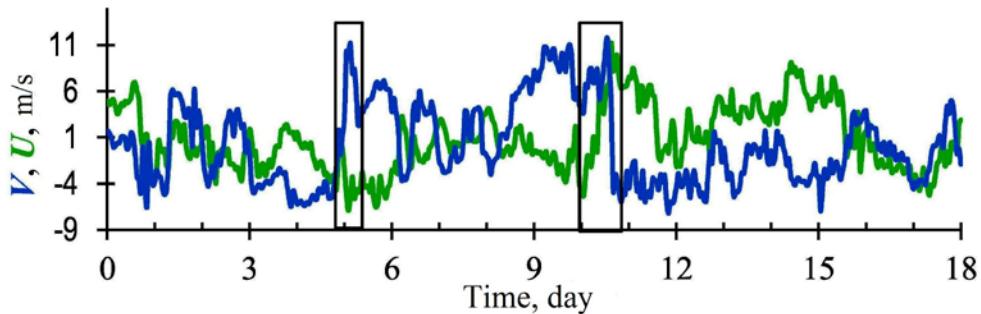


Fig. 1. Zonal V and meridional U projections of the wind speed vector during the typhoon evolution from August 20 to September 06, 2016

On the presented implementations of U and V , two characteristic features, highlighted by rectangles, are important for further presentation. The first of them occurs at midnight on August 25 and is associated with an intensive growth, a “gust” of the meridional wind velocity component U . For 6 hours, this velocity projection received an increment of ~ 20 m/s. The second feature occurs at noon on August 30 and is associated with a change in both the U - and V -projections. As in the case with the first feature, the meridional projection abruptly receives a negative increment of ~ 18 m/s. At the same time, the zonal projection of the wind speed receives the same increase in speed, but over a longer interval of ~ 12 hours. Thus, at noon on August 30, the wind direction changes from south to west, i.e. the wind speed vector acquired a cyclonic direction of rotation.

To study the inertial fluctuations in the velocity of currents in the Peter the Great Bay, we used the data from measurements performed by a Doppler current meter (ADCP) Aquadopp Profiler 400 kHz for the period from 00:00 on August 21 to 00:00 on September 7, 2016. The ADCP was located in the lower part of the surface buoy moored at a depth of 56 m in the southwestern region of the bay at a point with coordinates $42^{\circ}25'30''\text{N}$ and $130^{\circ}55'04''\text{E}$ in which the Coriolis parameter is equal to $f \sim 5.62 \cdot 10^{-2} \text{ h}^{-1}$. The ADCP directed downward recorded the flow profile in the layers of 4 m thick in the depth range from 2 to 45 m with 30 min discreteness and an accuracy of 0.5 cm/s in the velocity range of 3–250 cm/s. In Fig. 2, a schematic map of the study area is shown. The sign (\star) marks the location of the Seawatch system. The arrows indicate the near-slope jet Primorskoe current. The arrow on the compass marks the azimuth of this current in the area of the buoy during the impact of Typhoon Lionrock on the bay shelf waters.

For the current moment of time at fixed horizons, according to the ADCP measurements, the meridional v (per meridian) and zonal u (per parallel) projections of the current velocity vector were calculated. Then the realizations of the projections were smoothed by a low-frequency Tukey filter with a window of

36 h. The realizations $\langle v \rangle$, $\langle u \rangle$ of low-frequency pulsations with periods of 36 h and below, obtained after smoothing, served as a background for determining pulsations with variability in the range of 1.0–0.027 cycle/h. The latter were calculated as the difference between the background and initial realizations. The obtained series of fluctuations with mesoscale variability of the projections of the current velocity $v_1 = v - \langle v \rangle$ and $u_1 = u - \langle u \rangle$ were analyzed using the time-frequency spectral analysis.

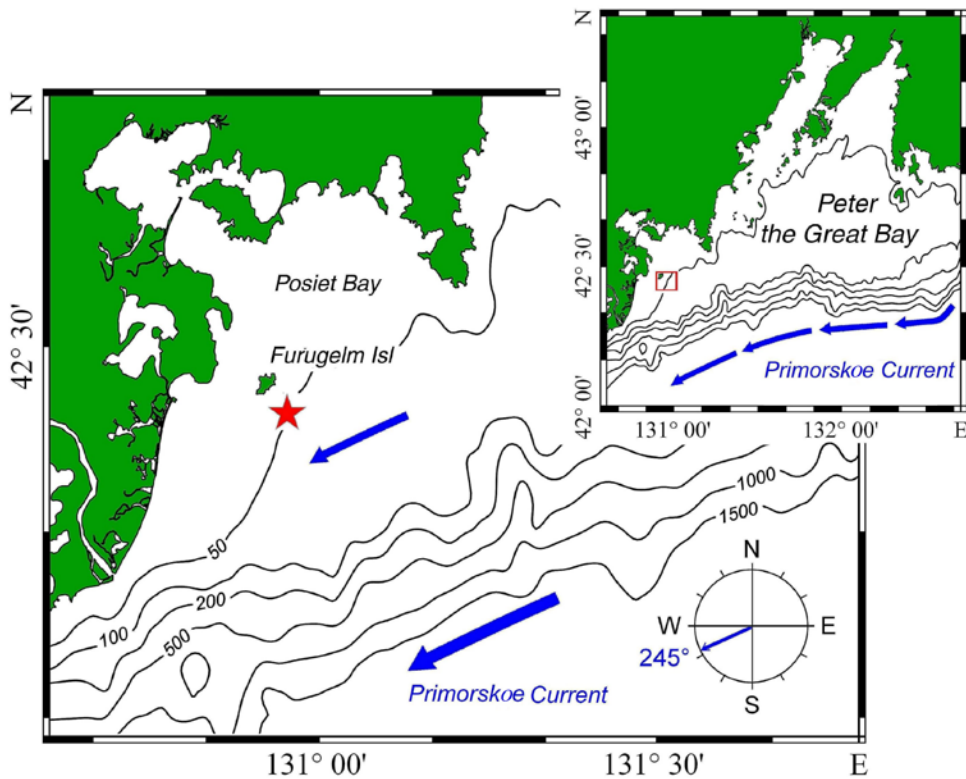


Fig. 2. Map of the region where the hydrographic buoy with the Seawatch measuring system was installed. Star denotes its location, and arrows – the Primorskoe current. The inset shows the Peter the Great Bay in the Sea of Japan [14, p. 94]

The paper [14] presents the results of calculations of the correlation coefficients ($r_{i, i+1}$) of the Primorskoe current velocity (u_1) on the neighboring horizons: z_i, z_{i+1} . It was found that with increasing distance between the horizons $r_{i, i+1}$ decreases, reaching a minimum of $r_{1.5} \sim 0.7$ between $z_1 = -4$ m, $z_5 = -24$ m, which indicates a strong positive relationship between velocity values at measurement horizons in the twenty-meter surface layer. Similar calculations $r_{i, i+1}$, were made for the velocity u_1 on the horizon $z_3 = -12$ m and adjacent horizons. It was determined that $r_{i, i+1}$ between u_1 at the horizon z_3 and adjacent horizons $z = -8$ m, $z = -16$ m is ~ 0.9 , and between z_3 and z_6 it is equal to -24 m, $r_{3, 6} \sim 0.8$. Thus, in the twenty-meter surface layer, the velocity u_1 is characterized by a strong positive relationship between the horizons. On this basis, we believe that the Primorskoe current at the horizon

$z_3 = -12$ m and the horizons adjacent to it quite completely characterizes the current in the active layer of the bay, and in the future, the characteristics of the current at this horizon are analyzed in the work.

Let us consider the characteristic features of the current in the observation region and the temporal variability of its velocity caused by the typhoon. As it is known, the azimuth of the Primorskoe current core is directed parallel to the continental slope and makes an angle of $\sim 245^\circ$ in the observation area [18]. The calculation of the velocity of this current was carried out according to the formula: $u_{pc} = u \cos \theta - v \sin \theta$, where u and v are the zonal and meridional projections of the current velocity vector; angle $\theta = -25^\circ$. In Fig. 3 the synoptic component (dashed curve) of the Primorskoe current velocity starting at 00:00 on August 20, 2016, against which its mesoscale fluctuations develop (solid curve) is represented.

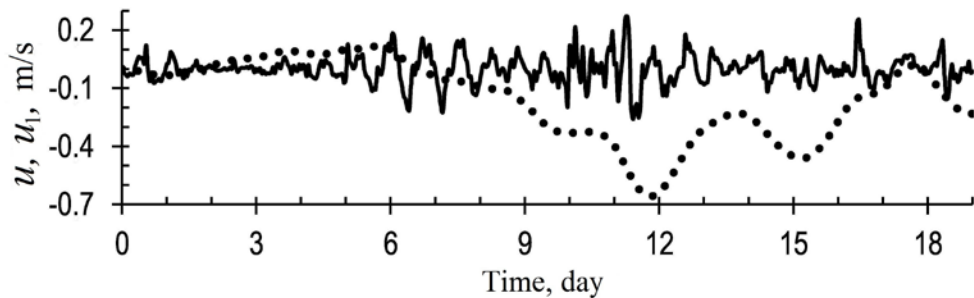


Fig. 3. Realizations of synoptic pulsations u (dotted curve) and mesoscale oscillations u_1 (solid curve) of the Primorskoe current velocity in the active layer of the Peter the Great Bay from August 20 to September 6, 2016

It follows from the Figure that from August 22 to 27, under the effect of the cyclone that entered the Sea of Japan water area, a slight increase in the flow velocity of the North Korean current with a slight anticyclonic vorticity took place. It should also be noted that mesoscale fluctuations in the u_{pc} velocity in this time interval, caused by a gust of wind at midnight on August 25, increased rapidly. At the phase of maximum development, the amplitude of these oscillations reached a value of 0.5 m/s, that is, it exceeded the amplitude of the synoptic pulsations highlighted in the figure by the dotted curve.

Subsequently, from August 27, under the effect of Typhoon Lionrock, the Primorskoe current begins to intensify, and during its maximum development, the value of the velocity of this current u_{pc} reached its maximum $u_{max} \sim 0.86$ m/s. It should also be noted that the intensity of mesoscale fluctuations in the u_{pc} velocity increased again in this interval. At the phase of maximum development, the amplitude of these oscillations again reached values close to 0.5 m/s, that is, it exceeded the amplitude of the synoptic pulsations highlighted in the Figure by the dotted curve. It should also be noted that a day earlier on August 31 between 13:00 and 14:00 a gust of wind of a significant intensity was registered again, which probably caused these fluctuations.

Thus, during the period of maximum development of Typhoon Lionrock in the area under study, according to [11, 12], there were favorable conditions for the manifestation of anomalous IO variability, including excitation of IO with non-standard counterclockwise rotation, i.e. with cyclonic direction of the velocity vector rotation.

The IO differ to a large extent, for example, from tides in their significant irregularity, that is, they are an example of a non-stationary process. Taking this feature into account, the IO analysis was carried out using the time-frequency spectrum $Sp(\omega;t)$ ². To construct it, monthly realizations of u, v velocity projections were divided into segments of equal duration with a shift of the beginning of each segment report by half the duration from the beginning of the previous segment. In this case, the duration of the initial segment was chosen to be equal to seven days, which is an approximate synoptic scale of atmospheric variability on the coast of the bay. Thus, the time interval of the typhoon evolution was divided into three periods: the initial period from August 21 to 28, the period of maximum development from August 24 to 31, and the final period from August 29 to September 4, 2016.

Further, for each period of the typhoon evolution, the spectral density of the kinetic energy of the zonal (S_{uu}) and meridional (S_{vv}) projections of the velocity vector, as well as their mutual spectrum Q_{uv} , were calculated using standard methods of spectral analysis. In this case, the main attention was paid to variations in the current velocity at frequencies from the inertial range: 1/12–1/24 cycle/h.

Using S_{uu}, S_{vv} and Q_{uv} , the spectral densities of rotational kinetic energy (RKE) were calculated: the anticyclonic component of the velocity vector Sp^- and the cyclonic component of the velocity vector Sp^+ . The spectral densities Sp^- and Sp^+ are the functions of the autospectra S_{uu}, S_{vv} and the quadratic spectrum Q_{uv} . At frequencies from the inertial range, the indicated spectra densities were determined by the formulas from [15]: $Sp^+ = (S_{uu} + S_{vv} + 2Q_{uv}) / 2$; $Sp^- = (S_{uu} + S_{vv} - 2Q_{uv}) / 2$.

An integral property of an inertial current is the rotation of its velocity vector, the direction of which is set by the coefficient $\sigma = (Sp^+ - Sp^-) / (Sp^+ + Sp^-)$. At $Sp^- > Sp^+$, the spectral density of RKE component with clockwise rotation exceeds RKE component with counterclockwise rotation, i.e. the condition $\sigma < 0$ is satisfied, which corresponds to the anticyclonic rotation of the velocity vector. In the opposite case, $Sp^- < Sp^+$, the coefficient $\sigma > 0$, therefore, the rotation of the velocity of this current occurs counterclockwise.

An important characteristic of inertial currents is the velocity hodograph of these currents, its shape and orientation. In the general case, the hodograph has an elliptical shape with major and minor axes L_M, L_m , respectively. The major and minor axes are calculated using the formula as $\sqrt{Sp^+} \pm \sqrt{Sp^-}$. In this case, the ellipse has an average orientation, the azimuth of which in relation to the zonal direction is calculated by the formula $2\psi = \arctg[2S_{uv} / (S_{uu} - S_{vv})]$, where ψ is set counterclockwise from the east direction.

² Dragan, Ya.P., Rozhkov, V.A. and Yavorsky, I.N., 1987. [*Methods of Probabilistic Analysis of Rhythms of Oceanological Processes*]. Leningrad: Gidrometeoizdat, 319 p. (in Russian).

Table 1

**Characteristics of inertial currents at the anticyclonic rotation direction
of shelf waters of the bay active layer at different stages
of the Typhoon Lionrock evolution**

Stage	$Sp_m^-, \text{cm}^2 \cdot \text{s}^{-2} \cdot \text{h}$	T, h	$L_M, \text{cm/s}$	$L_m, \text{cm/s}$	ε	ψ, degree
1	1800	18	57	28	0.48	33
2	640	18	45	6	0.12	-36
3	300	20	35	0.6	0.02	8

Table 2

**Characteristics of inertial currents at the cyclonic rotation direction of shelf waters
of the bay active layer at different stages of the Typhoon Lionrock evolution**

Stage	$Sp_m^+, \text{cm}^2 \cdot \text{s}^{-2} \cdot \text{h}$	T, h	$L_M, \text{cm/s}$	$L_m, \text{cm/s}$	ε	ψ, degree
1	300	16	53	19	0.36	23
2	640	16	44	6	0.15	24
3	431	18	37	5	0.13	27

The results of calculations of the listed characteristics of the current velocity inertial oscillations are presented in Tables 1 and 2. In the tables, lines 1, 2, 3 correspond to three stages of the typhoon impact on shelf waters: the initial stage from August 20 to 28 (line 1), the stage of maximum effect from August 28 to September 3 (line 2) and the final stage c 3 to 9 September (line 3). In the tables, Sp_m^- ($\text{cm}^2 \cdot \text{s}^{-2} \cdot \text{h}$), Sp_m^+ ($\text{cm}^2 \cdot \text{s}^{-2} \cdot \text{h}$) correspond to the maximum spectral energy densities of the IO velocity vector at periods T (h) with anticyclonic and cyclonic rotation directions, respectively. The tables present the values of the major L_M (cm/s) and minor L_m (cm/s) axes of the ellipse, as well as its eccentricity ε and the direction of its major semiaxis ψ , deg, relative to the meridional direction at three stages of the typhoon evolution.

Let us consider IO features in the upper quasi-homogeneous layer of the southwestern region of the Peter the Great Bay, as well as variability of the characteristics of these IO at different stages of Typhoon Lionrock evolution.

Discussion

In Fig. 4 the spectral densities of RKE components with cyclonic Sp^+ ($\text{cm}^2 \cdot \text{s}^{-2} \cdot \text{h}$) and anticyclonic Sp^- ($\text{cm}^2 \cdot \text{s}^{-2} \cdot \text{h}$) of rotation direction of mesoscale current velocity fluctuations at three stages of typhoon evolution are represented.

At the first, initial stage, which lasted from August 20 to 28, an increase in the synoptic component of the Korean current flow velocity (Fig. 3) and a southerly wind velocity gust, which caused anomalous mesoscale variability of the zonal and meridional projections of the current velocity vector, were recorded.

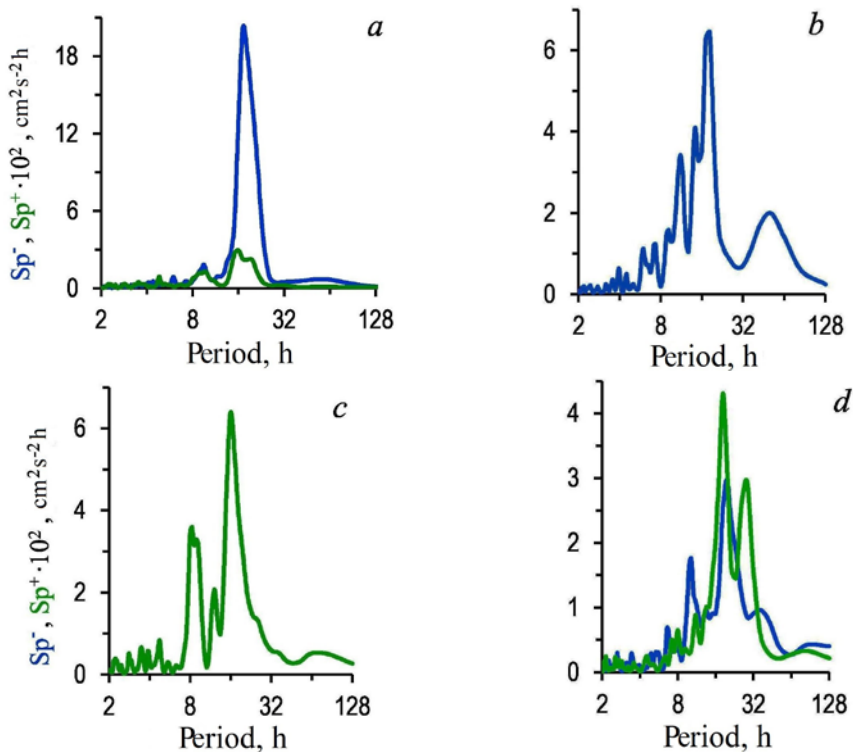


Fig. 4. Spectral densities of kinetic energy of the components at the clockwise Sp^- ($\text{cm}^2\cdot\text{s}^{-2}\cdot\text{h}$) (blue lines) and counterclockwise Sp^+ ($\text{cm}^2\cdot\text{s}^{-2}\cdot\text{h}$) (green lines) rotations at the following stages of the typhoon evolution: the initial (*a*), maximum (*b*, *c*) and final (*d*) ones

In Fig. 4, *a*, the spectral densities of RKE for the velocity vector component with the anticyclonic direction of rotation Sp^- and the components with the cyclonic rotation Sp^+ at the first stage of the typhoon evolution are shown. According to the Figure, Sp^- has a single peak shape with a maximum at the period $T_i \approx 18$ h/cycle, close to the period inverse of the Coriolis parameter $1/f \approx 17.8$ h/cycle. It is also easy to see that the spectral density of RKE of the anticyclonic component of the inertial current is almost an order of magnitude higher than the similar energy of the cyclonic component of the velocity vector of this current. Hence it follows that the rotation coefficient of the velocity vector at a frequency of $1/18$ cycle/h is less than zero, therefore, the rotation direction of this current is anticyclonic. The calculation of the ratio of the major L_M to the minor axis L_m of the velocity hodograph of this current was $L_m/L_M \approx 0.5$. Thus, the velocity hodograph of this current has an elliptical shape with an eccentricity $\varepsilon \approx 0.5$ and a semi-major axis rotated counterclockwise by an angle of $\sim 33^\circ$ relative to the zonal direction.

Let us consider the IO characteristics at the stage of maximum development of the typhoon, which lasted from August 28 to September 3. At this stage, the Primorskoe current flow velocity increased significantly to $0.9 \text{ m}\cdot\text{s}^{-1}$, the anticyclonic vorticity of its velocity increased, and the intensity of the wind

speed cyclonic component increased significantly, which caused a further increase in the mesoscale variability of the Primorskoe current velocity.

Fig. 4, *b* and *c* show the spectral densities Sp^- and Sp^+ with maxima at frequencies $\omega_i^- \approx 2\pi/18$ (rad/h) and $\omega_i^+ \approx 2\pi/16$ (rad/h) and similar values of RKE with opposite directions of rotation, respectively. Attention is drawn to a significant change in RKE distribution between two rotational components of the current velocity. If Sp^- declined by about fifty percent, then the similar energy of the cyclonic component Sp^+ increased by about an order of magnitude. Besides, the spectral densities Sp^- and Sp^+ acquired a two-peak shape with additional maxima at frequencies of $\omega_1^- \approx 2\pi/10$ (rad/h) and $\omega_1^+ \approx 2\pi/8$ (rad/h) close to the frequencies of the first subharmonics of each of the rotational components.

Significant changes also occurred with the hodographs of the velocities of the currents under consideration at the frequencies: ω_1^- and ω_1^+ . It was determined that the major semi-axis of the inertial current hodograph with an anticyclonic rotation direction with frequency ω_1^- is rotated by an angle $\psi \approx 36^\circ$ clockwise relative to the zonal direction, i.e. approximately along the normal to the Primorskoe current core. At the same time, the semi-major axis of the IO hodograph with the frequency ω_1^+ is rotated by an angle of 24° , that is, located almost parallel to the Primorskoe current core.

At the final stage (Fig. 4, *d*), which lasted from September 1 to 7, a decrease in the intensity of inertial oscillations of current velocity with the opposite direction of rotation was recorded against the background of a weakening of the Primorskoe current flow velocity. First of all, this applies to inertial currents with an anticyclonic direction of rotation. The maximum spectral density of RKE with this direction of rotation Sp_m^- from August 21 to September 7 decreased by about six times. During the same time, the maximum spectral density Sp_m^+ increased almost threefold, that is, the spectral densities of RKE of both the cyclonic and anticyclonic components of the inertial current excited by Typhoon Lionrock demonstrated an antiphase nature of variability.

In Fig. 4, *d*, the spectral densities of RKE with clockwise (Sp^+) and counterclockwise (Sp^-) rotation are represented. It follows from the Figure that Sp^- and Sp^+ at this stage retained their two-peak shape, but the position of their maxima changed. First of all, it should be noted that if at the previous stages the rotation of the velocity vector with a period of ≈ 18 h/cycle is anticyclonic, then at the final stage the velocity vector rotates counterclockwise with this period, that is, the direction of its rotation has changed to the opposite, cyclonic one.

Thus, at the final stage, the maximum of RKE spectral density, as before, is located at a frequency close to f , but the direction of the current velocity rotation has changed to the opposite cyclonic one. It should also be noted that the velocity hodograph of this current retained a quasi-elliptical shape, the major semi-axis of which exceeds the minor one by an order of magnitude, and the direction of this axis to the zonal direction made an angle $\psi \approx 27^\circ$, i.e. again, as in the previous two stages, it is close to the Primorskoe current midstream.

Let us use the IO model proposed in [12] against the background of a current with a constant velocity shear for a qualitative interpretation of some features of these currents recorded over the shelf of the Peter the Great Bay, excited by Typhoon Lionrock, keeping in mind that the background current with a velocity shear is the near-slope jet Primorskoe current intensified by the same typhoon.

According to the model, u , v are the meridional and zonal projections of the current velocity vector and satisfy the relations

$$u = -\alpha \left(y + \frac{q_x}{f} \right) + \frac{\alpha + f}{f} q_x \cos(ft) + \frac{\alpha + f}{f} q_y \sin(ft), \quad (1)$$

$$v = q_y \cos(ft) - q_x \sin(ft). \quad (2)$$

When deriving relations (1) and (2), it was assumed that at $t < 0$ the fluid moves in such a way that $u = -\alpha y$, $v = 0$, and at $t = 0$, a pulse action $q = (q_x, q_y)$ uniform in space and depth is applied to the fluid causing it to move.

From relations (1), (2) it follows that in the absence of a shear current, i.e. at $\alpha = 0$, the velocity vector at each point rotates in a clockwise direction with a frequency equal to the parameter f . The presented solution (1), (2) also shows that the current with a shear velocity, in contrast to the results of [19–21], does not affect the frequency of its velocity vector IO.

In accordance with the data from Tables 1 and 2, we came to a similar conclusion that at all stages of the typhoon impact on the near-slope Primorskoe current, the frequency of mesoscale oscillations of the velocity vector of this current in the inertial range against its background remains stable and close to the Coriolis parameter.

The velocity hodograph is one of the most important characteristics of inertial currents. In accordance with expressions (1), (2), the velocity hodograph of this current is set by the relation

$$\frac{u'^2}{(1 + \alpha f^{-1})} + v^2 = q_x^2 + q_y^2, \quad (3)$$

where $u' = u + \alpha y$ is a projection of the inertial current velocity vector onto the abscissa axis.

According to formula (3), the hodograph of inertial currents in the presence of a current with a velocity shear is an ellipse, the shape of which essentially depends on this shear. In other words, if the background current has a cyclonic vorticity that is equal to or exceeds the absolute value of the Coriolis parameter f , then the anticyclonic rotation of IO velocity vector is replaced by the opposite, cyclonic rotation. It is in this way that the authors of [10, 12] explain the rotation of IO velocity vector observed in some cases in the counterclockwise direction.

According to the measurement data, the Primorskoe current vorticity under the effect of the typhoon acquires a cyclonic character, changes and reaches a value that, apparently, exceeds the Coriolis parameter f . Against this background, under the effect of a gust of wind, the inertial oscillations are excited with a cyclonic direction by rotation of the current velocity vector, which was recorded by the Seawatch system.

Conclusion

We are to formulate the main results of the work. According to the measurements carried out via the Seawatch system, it was found that oscillations of current velocity vector with a frequency close to the Coriolis parameter, excited by Typhoon Lionrock in the southwestern region of the Peter the Great Bay, develop against the background of the near-slope Primorskoe current, significantly enhanced by the same typhoon. The spectral analysis of the rotational components of these current velocity fluctuations revealed the following:

- frequency stability, which accounts for the maximum spectral density of the kinetic energy of currents with rotation at a frequency close to the Coriolis parameter, at all stages of typhoon evolution;
- presence of inertial currents with counterclockwise rotation of their velocity vector, with the semi-major axis of the velocity hodograph of these currents parallel to the Primorskoe current core at all stages of the typhoon development;
- presence of subharmonics in the frequency of inertial oscillations of current velocity with both cyclonic and anticyclonic directions of rotation at the stages of maximum and final typhoon development.

The noted anomalous phenomena in inertial currents in the region of the Seawatch system deployment: stability of IO frequency, anomalous values of the eccentricity of IO velocity hodograph, change in the direction of rotation from the anticyclonic to the cyclonic one of the IO velocity vector – received a qualitative explanation within the framework of the model of inertial oscillations in the presence of a shear current. To interpret the non-stationary nature of the IO caused by amplitude modulation, as well as subharmonics of the frequency of these oscillations, it will apparently be necessary to use a nonlinear model of intense IO on a shear current.

REFERENCES

1. Kamenkovich, V.M. and Monin, A.S., eds., 1978. *Physics of the Ocean. Ocean Dynamics*. Moscow: Nauka. Vol. 2, 435 p. (in Russian).
2. Alford, M., 2001. Internal Swell Generation: the Spatial Distribution of Energy Flux from the Wind to Mixed Layer Near-Inertial Motions. *Journal of Physical Oceanography*, 31(8), pp. 2359-2368. doi:10.1175/1520-0485(2001)031<2359:ISGTSD>2.0.CO;2
3. Fu, L.L., 1981. Observations and Models of Inertial Waves in the Deep Ocean. *Reviews of Geophysics*, 19(1), pp. 141-170. doi:10.1029/RG019i001p00141
4. Price, J.F., 1983. Internal Wave Wake of a Moving Storm. Part I. Scales Energy Budget and Observations. *Journal of Physical Oceanography*, 13(6), pp. 949-965. doi:10.1175/1520-0485(1983)013<0949:IWWOAM>2.0.CO;2
5. D'Asaro, E.A., Eriksen, C.C., Levine, M.D., Paulson, C.A., Niiler, P. and Meurs, P.V., 1995. Upper-Ocean Inertial Currents Forced by a Strong Storm. Part I: Data and Comparisons with Linear Theory. *Journal of Physical Oceanography*, 25(11), pp. 2909-2936. doi:10.1175/1520-0485(1995)025<2909:UOICFB>2.0.CO;2
6. Olbers, D., Jurgenowski, P. and Eden, C., 2020. A Wind-Driven Model of the Ocean Surface Layer with Wave Radiation Physics. *Ocean Dynamics*, 70(8), pp. 1067-1088. doi:10.1007/s10236-020-01376-2

7. Bondur, V.G., Vorobjev, V.E., Grebenjuk, Yu.V., Sabinin, K.D. and Serebryny, A.N., 2012. Study of Fields of Currents and Pollution of Coastal Waters on Gelendzhik Shelf of the Black Sea with Space Monitoring Methods. *Issledovanie Zemli iz Kosmosa*, (4), pp. 3-12 (in Russian).
8. Bondur, V.G., Keeler, R.N., Starchenkov, S.A. and Rybakova, N.I., 2006. Monitoring of the Pollution of the Ocean Coastal Water Areas Using Space Multispectral High Resolution Imagery. *Issledovanie Zemli iz Kosmosa*, (6), pp. 42-49 (in Russian).
9. Keeler, R., Bondur, V. and Vithanage, D., 2004. Sea Truth Measurements for Remote Sensing of Littoral Water. *Sea Technology*, 45(4), pp. 53-58. Available at: http://www.aerocosmos.info/pdf/1/2004_Keeler_Bondur_Vithanage_SeaTech.pdf [Accessed: 02 April 2023].
10. Bondur, V.G., Sabinin, K.D. and Grebenyuk, Y.Y., 2013. Anomalous Variation of the Ocean's Inertial Oscillations at the Hawaii Shelf. *Doklady Earth Sciences*, 450(1), pp. 526-530. doi:10.1134/S1028334X13050012
11. Bondur, V.G., Sabinin, K.D. and Grebenyuk, Yu.V., 2015. Generation of Inertia-Gravity Waves on the Island Shelf. *Izvestiya, Atmospheric and Oceanic Physics*, 51(2), pp. 208-213. doi:10.1134/S0001433815020036
12. Sabinin, K.D. and Korotaev, G.K., 2017. Inertial Oscillations over the Background of Shear Currents in the Ocean. *Izvestiya, Atmospheric and Oceanic Physics*, 53(3), pp. 352-358. doi:10.1134/S0001433817030100
13. Gill, A.E., 1982. *Atmosphere-Ocean Dynamics*. New York: Academic Press, 397 p.
14. Novotryasov, V.V., Lobanov, V.B. and Sergeev, A.F., 2019. The Features of Inertial Oscillations in the Current Velocities in the Peter the Great Caused by Extreme Atmospheric Forcing (on the Example of Typhoon Lionrock). *Journal of Oceanological Research*, 47(3), pp. 92-103. doi:10.29006/1564-2291.JOR-2019.47(3).8 (in Russian).
15. Emery, W.J. and Thomson, R.E., 1998. *Data Analysis Methods in Physical Oceanography*. Pergamon, 634 p. doi:10.1016/C2010-0-66362-0
16. Astakhov, A.S. and Lobanov, V.B., eds., 2008. *Current Environmental Condition and Tendencies of its Change in the Peter the Great, Sea of Japan*. Moscow: GEOS, 460 p. (in Russian).
17. Lyubitsky, Yu.V., 2018. Storm Surge in Peter the Great (the Sea of Japan) from August 29 to September 2, 2016 Caused by the Lionrock Typhoon. *Vestnik of the Far East Branch of the Russian Academy of Sciences*, (1), pp. 31-39 (in Russian).
18. Yurasov, G.I. and Yarichin, V.G., 1991. *Currents of the Sea of Japan*. Vladivostok: Far Eastern Branch of the Russian Academy of Sciences Publishing, 176 p. (in Russian).
19. Fomin, L.M., 1973. [On Inertial Oscillations in the Horizontally Uneven Current Velocity Field in the Ocean]. *Izvestiya, Atmospheric and Oceanic Physics*, 9(1), pp. 75-83 (in Russian).
20. Mooers, C.N.K., 1973. Several Effects of a Baroclinic Current on the Cross-Stream Propagation of Inertial-Internal Waves. *Geophysics Fluid Dynamics*, 6(3), pp. 245-275. doi:10.1080/03091927509365797
21. Whitt, D.B. and Thomas, L.N., 2012. Near-Inertial Waves in Strongly Baroclinic Currents. *Journal of Physical Oceanography*, 43(4), pp. 706-725. doi:10.1175/JPO-D-12-0132.1

About the authors:

Vadim V. Novotryasov, Leading Research Associate, Department of Ocean and Atmosphere Physics, FSBSI POI FEB RAS (43 Baltiyskaya Str., Vladivostok, 690041, Russian Federation), Dr.Sci. (Phys.-Math.), Associate Professor, **ORCID ID: 0000-0003-2607-9290**, vadimnov@poi.dvo.ru

Aleksandr F. Sergeev, Senior Research Associate, Physical Oceanography Department, FSBSI POI FEB RAS (43 Baltiyskaya Str., Vladivostok, 690041, Russian Federation), sergeev@poi.dvo.ru

Elena P. Pavlova, Leading Engineer, FSBSI POI FEB RAS (43 Baltiyskaya Str., Vladivostok, 690041, Russian Federation), Ph.D. (Geogr.), epavlova@poi.dvo.ru

Contribution of the co-authors:

Vadim V. Novotryasov – formulation of the problem, qualitative and quantitative analysis of the results, writing the paper

Aleksandr F. Sergeev – execution of experimental work

Elena P. Pavlova – data preprocessing and analysis

The authors have read and approved the final manuscript.

The authors declare that they have no conflict of interest.